Chapter 5

Pruning front for the Hénon map

Our starting point, the pruning front picture of the once-folding map as defined by Cvitanović, Gunaratne and Procaccia [53] is in many ways equivalent to the multi-modal map picture. Assuming the pruning front description is correct, then this picture gives all admissible orbits of the map. Discrete approximations to the pruning front may be given as n-modal one-dimensional maps, and we show how one can describe the different n-modal bifurcations using the approximate pruning front. We will argue that the procedure we propose for defining a partition yields a unique partition for a pruned horseshoe map. The question of one unique partition is difficult and the discussion here should be regarded as the first step towards a rigorous treatment of this problem.

5.1 Symbol plane

The pruning front conjectured in ref. [53] is defined in a two dimensional symbol plane $(\delta, \gamma) \in ([0,1],[0,1])$. While ref. [53] uses coordinates (x_t, y_t) and (γ, δ), we prefer to use coordinates (x_t, x_{t+1}) and (δ, γ) because they simplify the comparison with the n-modal discussion. The coordinate γ is defined in (3.4); and coordinate δ is defined in (3.5) for a Smale horseshoe without reflection ($b < 0$ in the Hénon map), and in (3.6) for the Smale horseshoe with reflection ($b > 0$ in the Hénon map).

For the full Smale horseshoe the Cantor set in (x_t, x_{t+1}) is mapped uniquely by the rules above into the the symbol plane, preserving the phase-space topological ordering. We will now use this symbol plane to also describe the pruned horseshoe map.

5.2 Primary turning points

The main problem in the definition of the pruned horseshoe symbol plane is the choice of the symbol s_t corresponding to a phase space point (x_t, x_{t+1}) for the given parameters.

In the n-th one-dimensional approximation of the once-folding map we chose the symbols $s_t = 0$ if x_t lies to the left of the critical point and $s_t = 1$ if x_t lies to the right. The critical point is the the point where $dx_{t+1}/dx_t = 0$ and an important question is how many critical points we have for a given approximation and how this number changes. The complete horseshoe map has 2^n critical points but it may be less critical points in the pruned horseshoe.

We found that in the three-modal one-dimensional map in section 2.2 we had a bifurcation changing the modality from three to one. In the three-dimensional symbolic parameter space this bifurcation happens at two planes drawn in the figures 2.13, 2.17 and 2.20. In figure 2.16 a) and c) the function has three critical points and orbits are described by a four letter alphabet while in figure 2.16 b) the map is unimodal and a two letter alphabet describes all orbits. The typical bifurcation of periodic orbits are the cusp bifurcations discussed in section 2.2. The bifurcation changing modality creates difficulties when we want a complete description of all the bifurcations in one-dimensional map given by a polynomial of degree n.

For the four-modal approximation of the Hénon map discussed in section 4.4 we found a bifurcation from a four-modal map to a bimodal map for kneading sequences given in proposition 3. The border of the four-modal symbolic parameter space is a three-dimensional space which in a two-dimensional parameter space like (a, b) for the Hénon map, is a curve sketched in figure 4.40. This give the cusp bifurcations we found numerically for the Hénon map. Any higher modal approximation to the once-folding map has bifurcations decreasing the modality of the map.

To understand this changing of modality seems to be essential when we want to describe the pruned once-folding map by symbolic dynamics in an exact description.

In the Hénon map there can be no critical points in the strict one-dimensional map sense since $\det \mathbb{J} = b$ is constant, and no derivative vanishes for $b \neq 0$. Here the points that play a role similar to the critical points of one-dimensional maps are the *turning points* of the unstable manifold W^U, defined as points where the stable manifold W^S and the unstable manifolds W^U are parallel. If the attractor is chaotic then the turning points are identical to the homoclinic tangencies of W^S and W^U. If there are stable periodic orbit some turning points are in the basin of attraction. If the map is a repellor then some turning points are in the basin of

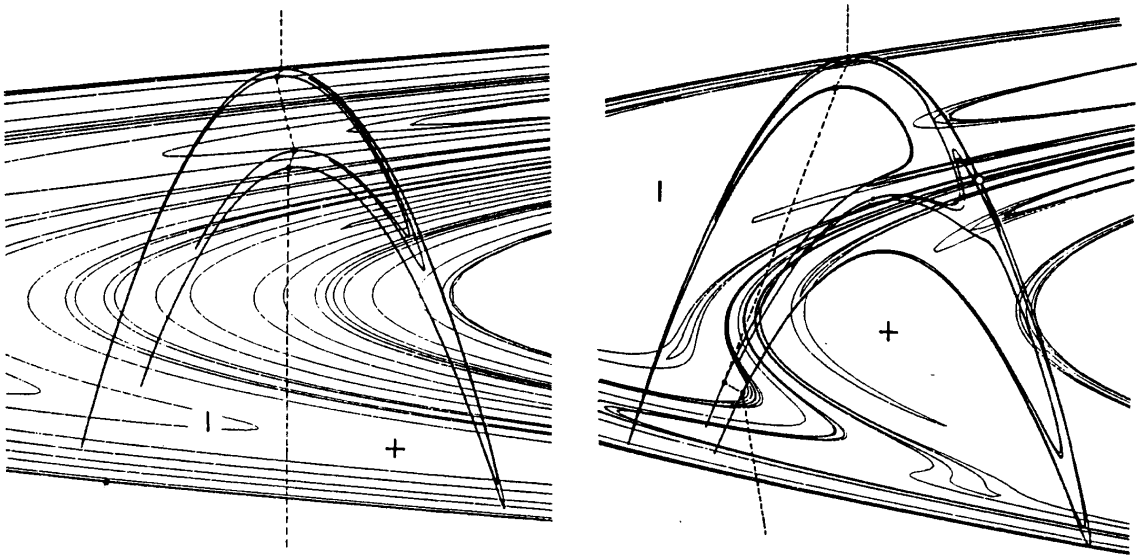

Figure 5.1: The Grassberger-Kantz partition line for the Hénon map for parameters a) $a = 1.4$, $b = 0.3$; b) $a = 1.0$, $b = 0.54$. From ref. [92].

attraction of infinity.

Grassberger and Kantz [92] have proposed that the "primary" homoclinic tangencies (turning points) generate a partition of the Hénon map. One of the images or preimages of a turning point has to be chosen as the primary turning point; according to Grassberger, Kantz and Moening [93] this choice is "...of course arbitrary, as all (pre-)images are equally good candidates".

We shall introduce here a prescription for determining which (pre-)images of the turning points that should be taken as primary and we believe this prescription is unambiguous.

In figure 5.1 the Grassberger-Kantz partition of the Hénon map is plotted for Hénon parameters $a = 1.4$, $b = 0.3$, and for the parameters $a = 1.0$, $b = 0.54$. In ref. [93] Grassberger, Kantz and Moening compare their partition to the partition obtained by the symbols of periodic orbits found using the real version of the Biham-Wenzel (BW) method (4.49). They find that their choice and the BW method give the same partition for $= 1.4$, $b = 0.3$, while for $a = 1.0$, $b = 0.54$ they get a different partition drawn in figure 5.2. The two partitions give the same entropy and the different symbols can be translated into each other by a finite set of substitution rules up to the given accuracy. However, we shall now argue that a partition different from both these two are preferable for reasons given below. This partition is indicated in figure 5.3.

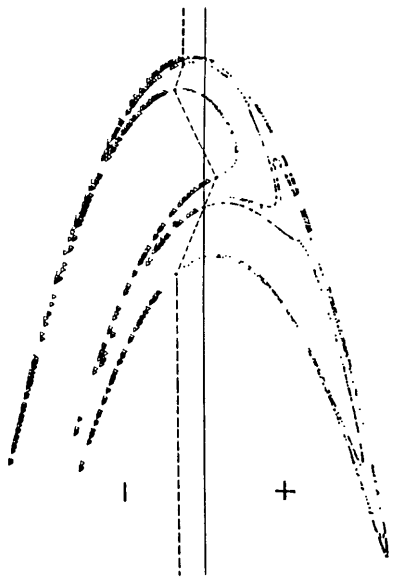

Figure 5.2: The partition line for the Hénon map for parameters $a = 1.0$, $b = 0.54$ calculated by the BW-method. From ref. [93].

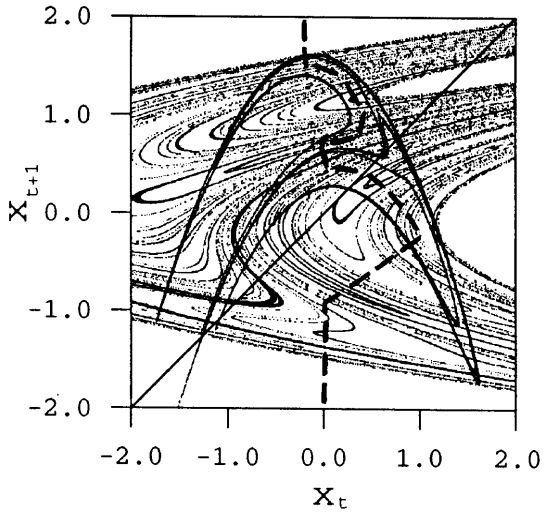

Figure 5.3: The partition line for the Hénon map for parameters $a = 1.0$, $b = 0.54$, constructed by the algorithm proposed here.

5.2.1 Bifurcations of turning points

We define a primary turning point (PTP) for the complete smooth Smale horseshoe map to be a point on one fold of W^U (the unstable manifold) at the point where this fold of W^U is parallel to the closest fold of W^S (the stable manifold) and the point has to be in the primary bent region of the horseshoe; in $g(Q)$ close to to middle of $g(Q)$ above Q in figure 3.1. For non-smooth maps like the Lozi map a PTP is at the point on W^U where the fold turns. In the Lozi map this is the line $x_t = 0$.

Each fold in the complete Smale horseshoe has one PTP, and each PTP has an infinite number of images and preimages that are turning points (TP) which are not primary. All the images of a PTP are below Q in figure 3.1, while the preimages of a PTP are in Q.

We choose some physical realization of the complete Smale horseshoe, e.g. the Hénon map, and then change smoothly the parameters. The number of TPs and folds in the Hénon map may be less than in the complete horseshoe. The folds changes smoothly with the parameters and we can study the bifurcation removing a TP. The bifurcation creating (or removing) a tangency between two given folds of W^U and W^S is much studied in mathematical literature and is very important

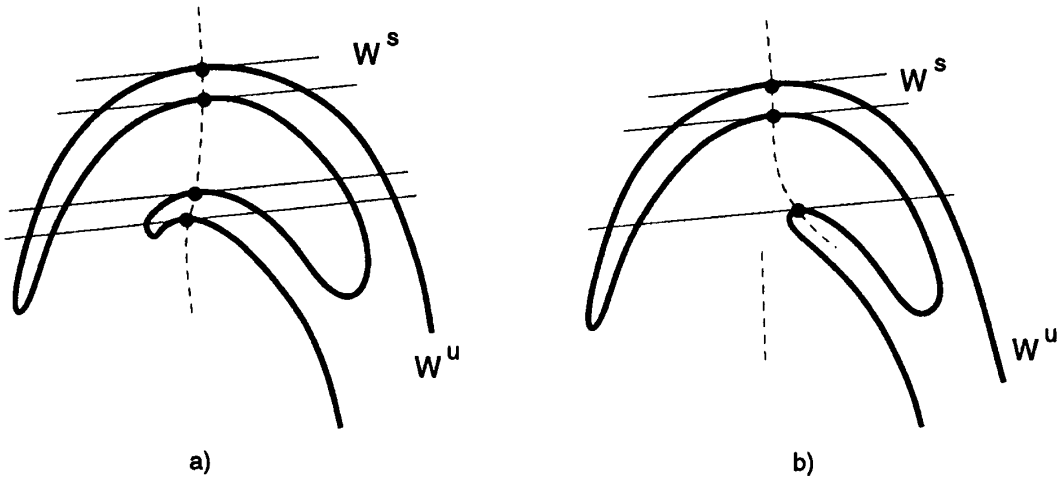

Figure 5.4: A partition of the once-folding map under a bifurcation of TPs that gives a discontinuous partition line.

in proving the Newhouse phenomena [160, 100] and in proving that a subset of the non-wandering set is given by a complete horseshoe. In these discussions the turning point exists both before and after the bifurcation and the bifurcation creating a TP is a different and much less studied bifurcation [115, 116]. We want to use PTPs as the partition giving symbolic dynamics. To understand how the symbolic dynamics change when we smoothly change the parameters we have to examine the bifurcation of TPs.

A simple way to describe the bifurcations appears to be to claim that when one PTP vanish this does not affect any other PTP. This is illustrated with the bifurcation sketched in figure 5.4: the thin lines are folds of W^S, the thick lines are folds of W^U and the dashed line is the partition line. The partition line we have in figure 5.4 b) through the three remaining PTPs are not continuous through the whole W^U. The partition line goes into one fold and has to continue outside this fold. In the limit $b \to 0$ for the Hénon map this partition does not approach a simple line through the critical point of the parabola. This is also not consistent with choosing $x = 0$ as the partition line for the Lozi map.

We find it necessary to choose a different and more complicated way to describe the partition line under a bifurcation of a PTP.

Assume that the fold A of W^U in figure 5.5 a) has three TPs labeled 1, 2 and 3 where TP no 2 is a PTP and that after n iterations of these folds of W^U and W^S we have the folds in B where TP 1 and TP 3 are PTPs. The partition line is drawn through TP 2 in A and TP 1 and TP 3 in B. As we change parameters

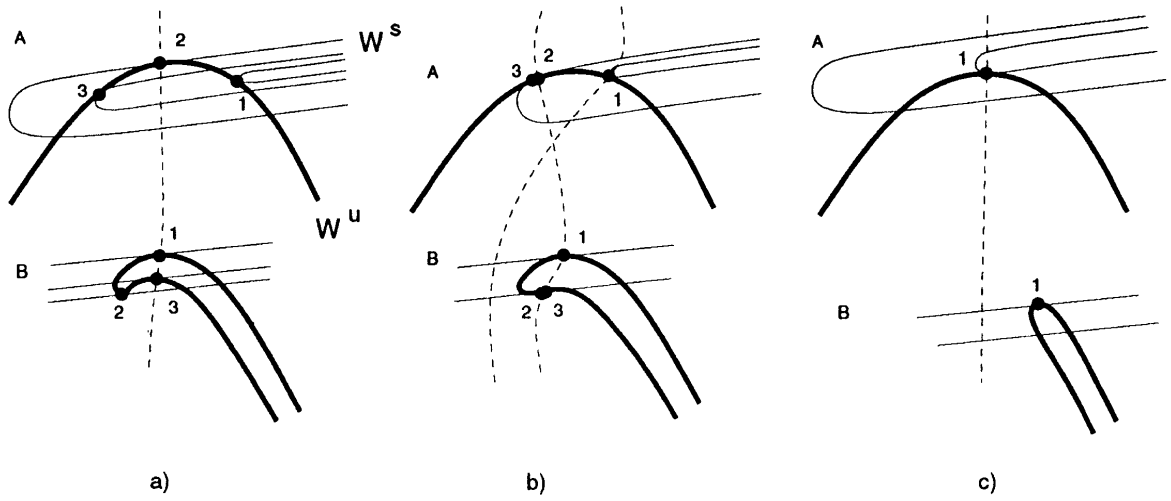

Figure 5.5: Bifurcation of the primary turning points of the once-folding map.

the two TPs 2 and 3 move closer and in figure 5.5 b) the two points disappears in of flip bifurcation. When only TP 1 is left in figure 5.5 c), we choose to draw the partition line through TP 1 at fold A of W^U and not through TP 1 at fold B. *At the bifurcation point we change which image of turning point 1 we consider primary from the point on fold B to the point on fold A which is its n-th preimage.* We claim that this is a general picture of the bifurcations of TPs and state the following conjecture.

Conjecture 1 *If there is a bifurcation where a TP disappears then there is always two TPs merging together and one can always find a (pre-)image A where one of the TPs is primary. One can also find a (pre-)image B where the second of the two TPs is primary and where the fold of W^S has a third TP which is primary in B. After the bifurcation the third TP is primary in A and not in B. This gives a continuous partition line and the partition is uniquely changing moving through the parameter space for all TPs that exist all along this path.*

That the partition line will be continuous follows because each folded part of W^U have either two PTPs or no PTPs and the folds of W^U is not dense in the phase space so two PTPs on neighbor folds of W^U can be connected by a curve. We have not managed to proof that the partition is unique when moving along different paths in the infinite dimensional parameter space but the example below suggests that this is the case. At the inflection point there may be created more than two TPs but it will be an even number of points and we can let two and two of the TPs bifurcate together.

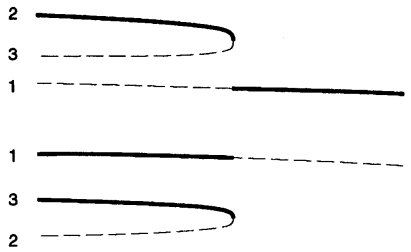

Figure 5.6: The bifurcation of primary (solid lines) and not primary (dashed lines) turning points as a function of a parameter.

The bifurcation in figure 5.5 is sketched as a function of a parameter in figure 5.6 with the same labeling of the turning points.

In figure 5.7 we show one numerical example for the Hénon map of this type of bifurcation. In this example fold B of W^U is above fold A in the phase space and fold B is the 3rd iterated of A such that the folding of B is modest. In figure 5.7 a) the down-most fold has the three TPs as in figure 5.5 a) fold A. In figure 5.7 b) a part of the uppermost foliation of figure 5.7 a) is magnified and we find the fold B which also has three turning points. The figures 5.7 c) and 5.7 d) show the manifolds at parameter values close to the bifurcation and in figures 5.7 e) and 5.7 f) there is only one PTP on the folds we are looking at. The partition line has jumped where it crosses fold A. Fold B is here on the right side of the partition line.

The most important bifurcation of this type is the one illustrated in figure 5.8 a) which give the bifurcation of the folds $\ldots 100s$ and $\ldots 101s$. This is the bifurcation giving the cusp structure in the examples of chapter 4. We follow the same principle in this case: the bent fold B moves to the left of the partition line and the partition line on fold $\ldots 10s$ jumps. This gives a partition which is not the one chosen by Grassberger and Kantz or the one the BW-method gives for parameters $a = 1.0$, $b = 0.54$. Instead it gives the one we indicated in figure 5.3.

Figure 5.8 b) illustrates a variation of the same bifurcation. In figure 5.5 we assumed that W^U is dense in the phase space such that the bifurcation is happening when the two turning points 1 and 2 are close in the phase space. This bifurcation may take place inside a basin of attraction. We are only interested in describing the non-wandering set and therefore is the bifurcation drawn in figure 5.8 b) of more interest than the point where the folding vanishes. In figure 5.8 b) the bifurcation is where the fold of W^U is tangent to the fold of W^S on the border of the basin of attraction. In figure 5.8 b) the turning points 1 and 3 is in the basin of attraction of ∞ and the of interest bifurcation takes place when also the turning point 2 moves out in the basin of attraction of ∞.

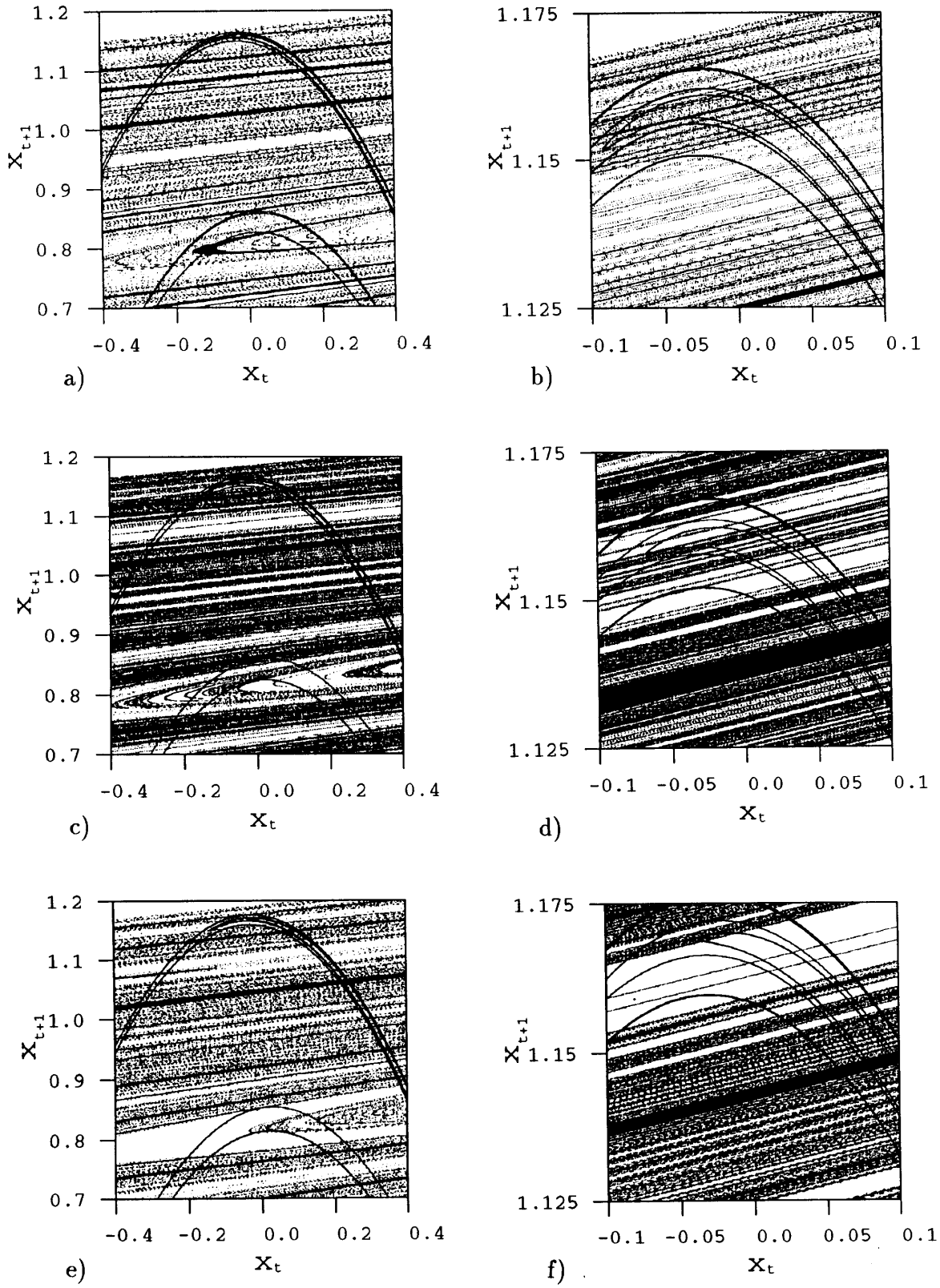

Figure 5.7: Bifurcation of the primary turning points of the Hénon map map. a) and b) $a = 1.6$, $b = 0.2$; c) and d) $a = 1.571$, $b = 0.2$; e) and f) $a = 1.562$, $b = 0.21$. b), d) and f) are magnifications.

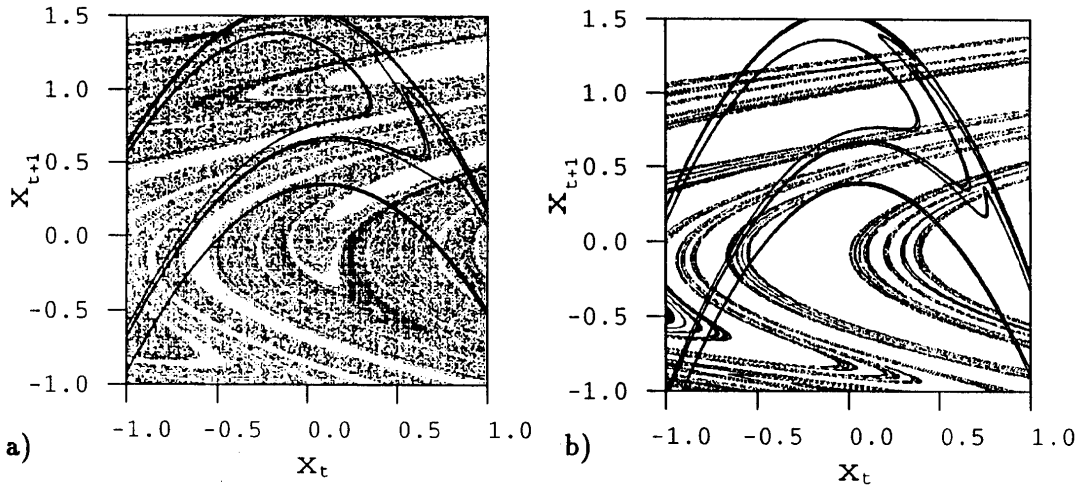

Figure 5.8: Bifurcation of a primary turning points of the Hénon map map. a) $a = 1.1$, $b = 0.522$; b) $a = 1.5$, $b = 0.58333$.

We examine some possible bifurcations in figure 5.9 to show how the mechanism of changing PTPs works in more complicated cases, and to investigate the uniqueness of the partition. Figure 5.9 a) and b) shows the same bifurcation as figure 5.5. The only differences is that we have drawn W^U as a straight line in A and we have added a new iteration C of the manifolds. In C none of the TPs are primary. In figure 5.9 c) there are 5 TPs and by pruning TP 4 and TP 5 from figure 5.9 c) we get figure 5.9 b). Notice that before the bifurcation TP 1 and TP 4 are primary in image C and TP 5 is primary in image B. The bifurcation changes TP 1 from being primary in C in figure 5.9 c) to be primary in B in figure 5.9 b). In figure 5.9 d) there are 7 TPs. The two TPs 6 and 7 can bifurcate together and we then after the bifurcation have the picture in figure 5.9 c). We have here a rather complicated foliation but in the bifurcation from figure 5.9 d) to figure 5.9 c) we are only interested in the fold with TP 3, TP 6 and TP 7. In figure 5.9 d) TP 6 is primary in B and TP 3 and TP 7 are primary in C. At the bifurcation TP 3 has to change from being primary in C to be primary in B which is the case in figure 5.9 c). These pictures describe a parameter path taking us from figure 5.9 d) to figure 5.9 a) through three bifurcations of turning points.

The figures 5.9 e) and f) show steps along another possible path in the parameter space changing figure 5.9 d) into figure 5.9 a). Instead of removing TP 6 and TP 7 from figure 5.9 d) we can remove TP 2 and TP 4 in a bifurcation. This give figure 5.9 e) and change TP 7 from being primary in C to be primary in A. From figure 5.9) we can have a bifurcation removing TP 6 and TP 7 giving figure 5.9 f)

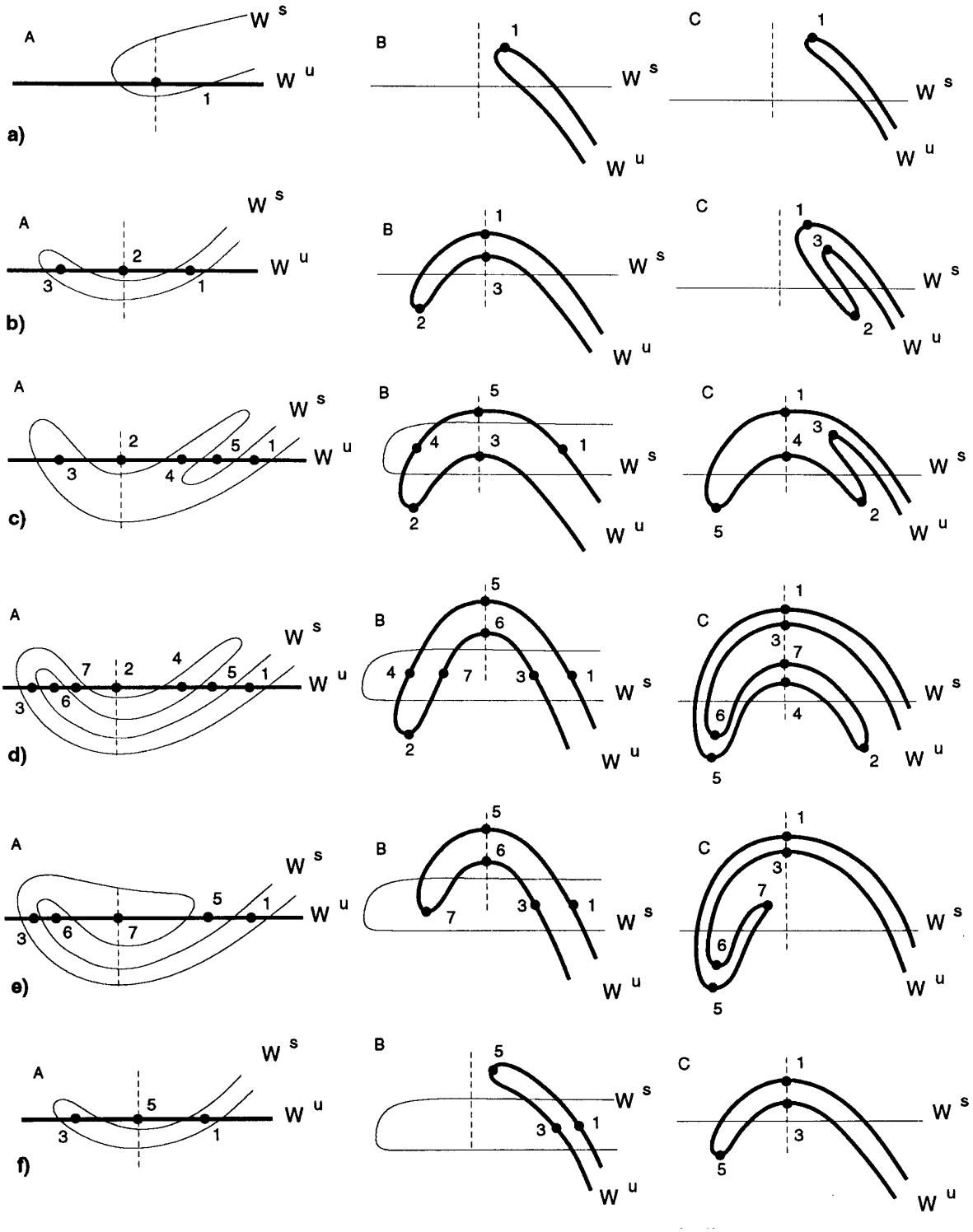

Figure 5.9: Different bifurcations of TPs in the once-folding map.

and we find that this change TP 5 from being primary in B to be primary in A. The figure 5.9 f) can be compared with figure 5.9 b) since both have three TPs but they are different since one TPs is different and the TPs are primary on different folds. By letting TP 3 and TP 5 in figure 5.9 f) bifurcate together we obtain figure 5.9 a) again and TP 1 will again be primary in A.

The path d)→c)→b)→a) changed TP 1 from being primary in C to be primary in A. The path d)→e)→f)→a) also changed TP to be primary in A. If the last path had given A primary in B or C this would have contradicted the uniqueness of the conjecture.

One bifurcation which can make the discussion more complicated is if one fold outside a second fold looses its PTP. This is unlikely to happen but if this happens we have to include more iterations of the innermost fold such that the PTPs on this folds jumps. In our example this would be the case if 4 and 5 bifurcated in figure 5.9 d).

Independent investigation has been done by Giovannini and Politi [85]. They have used a numerical method to investigate bifurcations of the PTP in the Hénon map and they use the point where the curvature is largest to define a PTP. They find that the PTP can jump when changing parameters in the way discussed here. They also discuss the case where the period 6 orbit changes symbolic description presented in ref. [107] and they conclude that the definition of which turning points that are primary is ambiguous and propose a pragmatic trial-and-error procedure. We suggest here that the definition of the primary turning points in the Smale horseshoe and the procedure to change the primary point each time there is a bifurcation gives a rigorous and unambiguous definition of all primary turning points. This procedure may however not be so useful in numerical studies but the principle may be combined with a numerical method like the one of Giovannini and Politi.

A consequence of our definition is that not only Does a PTP have a possibility to jump but it will jump each time the fold of W^U moves through a fold of WS. Because the turning points are bent sharply after some iterations for $|b|$ not too close to 1, most of these jumps are very small and not numerically detectable. This makes a discussion of an adiabatically change of a PTP more difficult.

5.3 Pruning front

Running a long orbit and plotting the (δ, γ) points for each iteration gives the figure 5.10 using the partition of Grassberger and Kantz $a = 1.4$, $b = 0.3$. The white region in the symbol plane is the symbolic values which no points in the

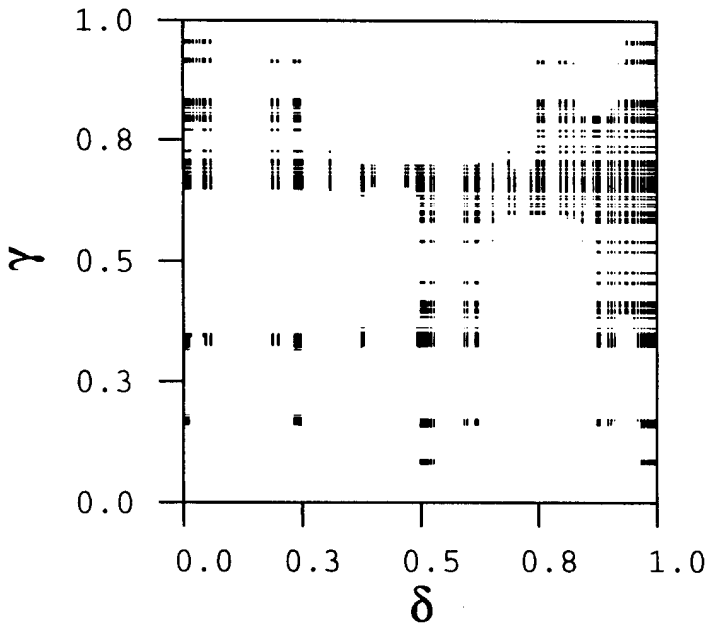

Figure 5.10: The chaotic orbit for $a = 1.4$, $b = 0.3$ plotted in the symbol plane.

chaotic attractor gives and these are the symbolic plane representation of the non existing orbits in the non-wandering set. We call this the forbidden regions of the symbol plane. Cvitanović et al. conjectured that in a plot like this (they plotted the unstable periodic orbits) the primary forbidden region is limited by the symbolic values (δ, γ) for the primary turning points. All forbidden regions are the primary forbidden region or a (pre-)image of this primary region. The border line is called the pruning front by Cvitanović et al. [53], and we also call the primary forbidden region in the symbol plane the primary pruned region.

In general is the pruning front a complicated monotone staircase curve but we can first investigate a simple example where the pruning front is an exact description of the non-wandering set.

5.3.1 Period 5

In figure 5.11 the stable and the unstable manifolds are plotted for the parameter values $a = 1.46$, $b = 0.17$. This are parameters inside the swallowtail crossing in figure 4.11 where the period 5 orbit is stable and in the two unimodal maps approximations the orbit has two points close to the two critical points. In figure 5.11 we find all turning points inside the basin of attraction for the period 5 orbit. This imply that the repellor is a hyperbolic set, a complete Smale horseshoe with a com-

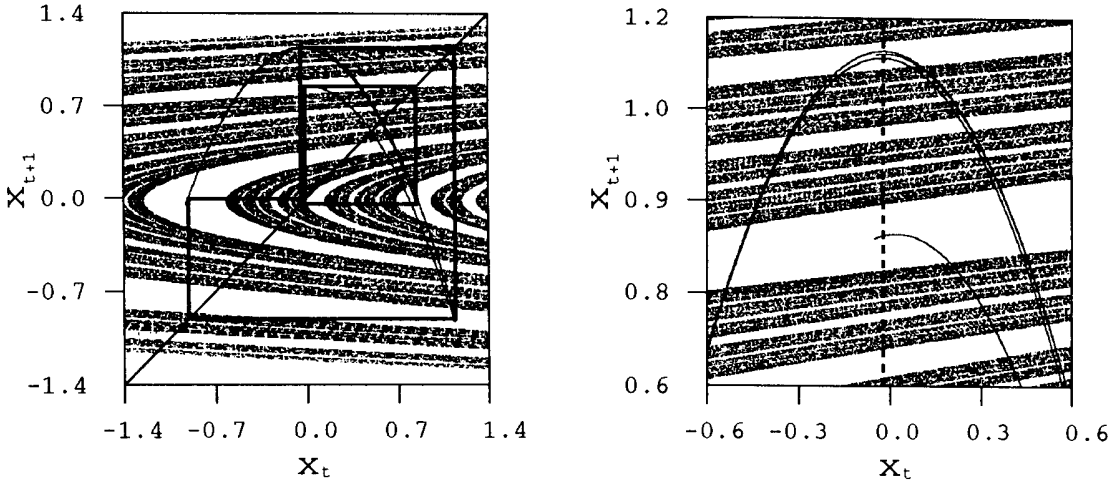

Figure 5.11: The stable and unstable manifolds and the stable period 5 orbit for $a = 1.46$, $b = 0.17$.

plicated folding. The repellor is plotted in the (x_t, x_{t+1}) plane in figure 5.12 and in the symbolic plane (δ, γ) in figure 5.13. We choose symbols according the the partition line indicated in figure 5.12. We want to describe the repellor and any partition curve crossing the unstable manifold in this basin of attraction gives the same symbolic dynamics for the repellor.

The symbolic strings which give the pruning front is the description of the unstable period 5 orbit. In figure 5.13 we have also plotted symbolic values for the four period 5 orbits; $\Box$ for $\overline{10111}$, $+$ for $\overline{10110}$, $\times$ for $\overline{10010}$ and $\triangle$ for $\overline{10011}$. We have plotted (δ, γ) only for the two cyclic permutations giving $\tau_0^{\max}$ and $\tau_1^{\max}$. In figure 5.13 we find that the values of γ $(= \tau)$ for the orbit $\overline{10111}$ gives the two maximum values the points of the repellor has. We have here an exact pruning front which is

$$\begin{aligned} \gamma &= 0.\overline{11010} \quad \text{for} \quad \delta \in (0, 1/4) \cup (3/4, 1) \\ \gamma &= 0.\overline{10110} \quad \text{for} \quad \delta \in (1/4, 3/4) \end{aligned} \tag{5.1}$$

In the symbolic parameter plane for the bimodal approximation this is the point $(\kappa_0, \kappa_1) = (0.\overline{10110}, 0.\overline{11010})$ and the approximation is exact in this case. This is the point in the corner of the swallowtail in the symbolic parameter plane in figure 4.10.

In figure 5.14 we have plotted the forbidden region and some of its images obtained by the shift operation. We find that the pruning front maps into the pruning front under iterations in the future which imply a finite markov partition. This is a consequence of that the pruning front is on periodic orbits.

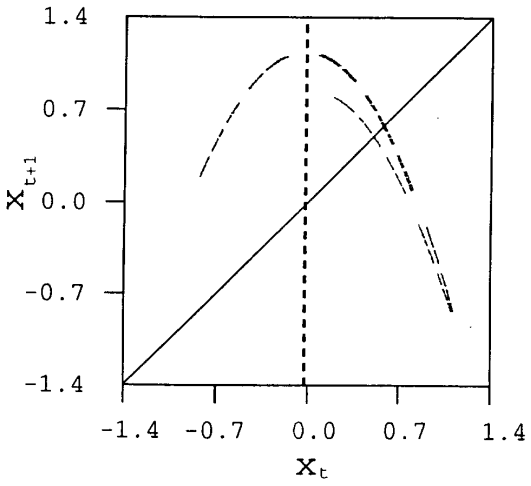

Figure 5.12: The repellor plotted in phase space (x_t, x_{t+1}) with the partition line defining symbols for $a = 1.46$, $b = 0.17$.

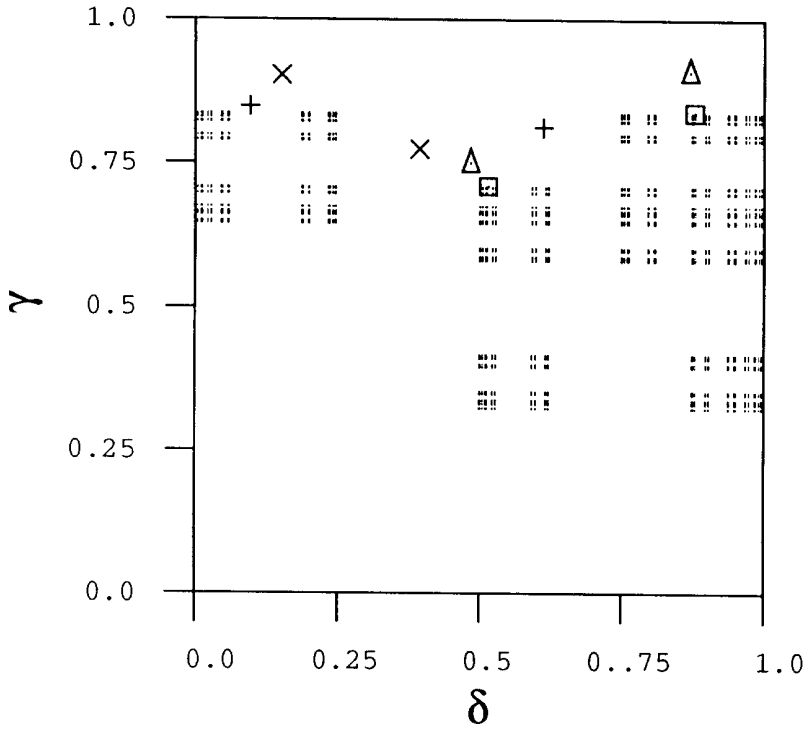

Figure 5.13: The repellor plotted in the symbol plane for parameters in the period 5 swallow tail crossing. The markers are : □ $\overline{10111}$, + $\overline{10110}$, × $\overline{10010}$ and △ $\overline{10011}$.

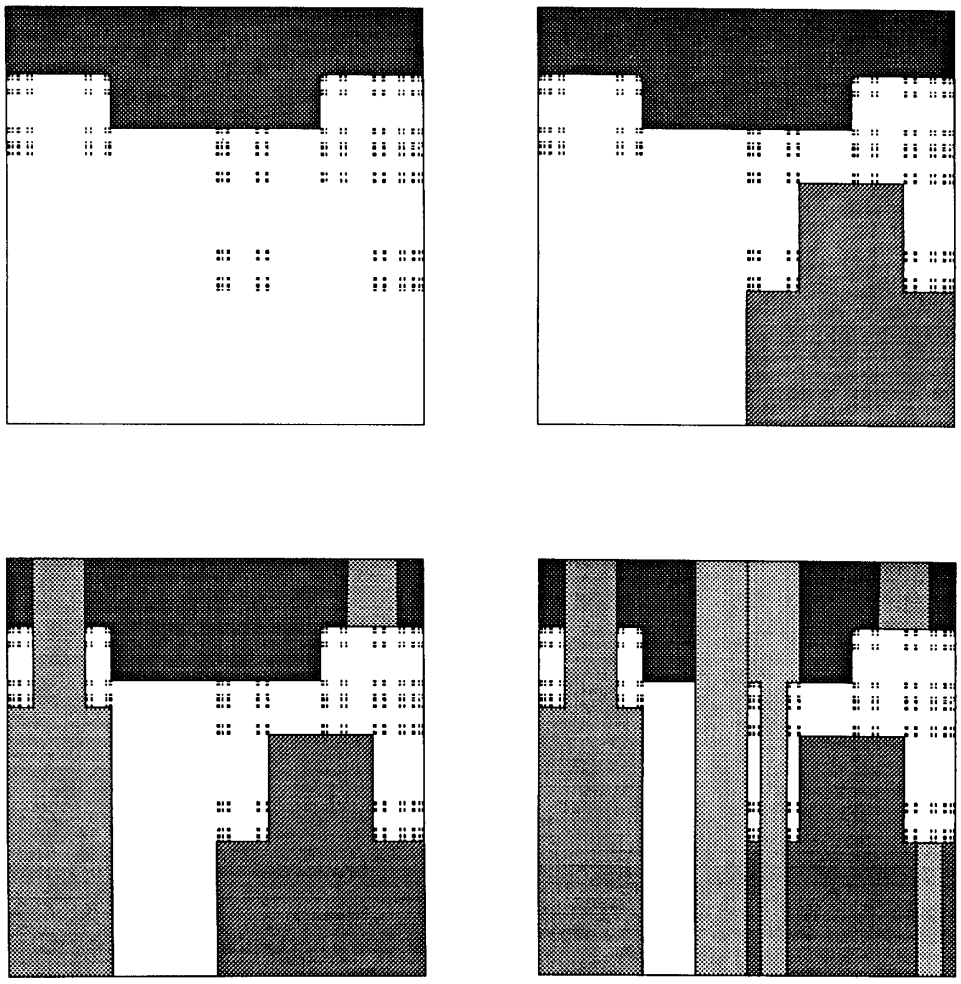

Figure 5.14: The primary forbidden region and its images.

In fact in this special case where we have a swallowtail crossing we only need one pruning front to describe the repellor because the step with the largest value $\gamma = 0.\overline{11010}$ maps onto the smaller value in the region above the non-wandering set as showed in the forth iteration in figure 5.14. The jump of the turning point here only affects the stable orbit which we know has to change symbolic description.

In other cases where a two step pruning front is exact, like the stable period 3 and stable period 5 orbit for parameters $a = 1.8125797$, $b = 0.0228643$ discussed in ref. [53] the front cannot be reduced to a one step front.

We can now use the two step pruning front to describe the bifurcation giving the period 5 swallowtail. The assumption we do is to assume that the pruning front only has two steps for all parameter values. If both steps have the same γ value and we let it decrease from 1.0, the pruning front passes through the markers in figure 5.13 in the order $\overline{10011}$, $\overline{10010}$, $\overline{10110}$ and $\overline{10111}$. These bifurcations give the two windows $\overline{1011\epsilon}$ and $\overline{1011\epsilon}$. Let then γ for the step $\delta \in (0, 1/4) \cup (3/4, 1)$ decrease while γ for $\delta \in (1/4, 3/4)$ is fixed at 1.0. Then the pruning front passes the markers in the symbol plane in the order $\overline{10110}$, $\overline{10010}$, $\overline{10011}$ and $\overline{10111}$ and this is the two windows $\overline{1010\epsilon}$ and $\overline{1110\epsilon}$. When we let both steps in the pruning front decrease we obtain the situation in figure 5.13. This is the same result as we obtained in the discussion with the approximation of a bimodal map. The bimodal approximation is identical to approximation the pruning front with two steps.

5.3.2 4 modal approximation

We can now easily see the connection between the multi-modal map description and the pruning front. The symbolic past of the point x_0 that is used to determine the value δ is the same symbols that we used to determine which map a point was on in the bimodal, four-modal, eight-modal, etc. approximation. In the bimodal approximation a point x_t is on map 1 if $s_{t-1} = 1$ which corresponds to that $\delta \in (0, 1/4) \cup (3/4, 1)$. A point on map 0 has $s_{t-1} = 0$ and therefore $\delta \in (1/4, 3/4)$. The two map approximation then corresponds to a pruning front with only two values; $\gamma = \kappa_1$ in the intervals $\delta \in (0, 1/4) \cup (3/4, 1)$ and $\gamma = \kappa_0$ in the interval $\delta \in (1/4, 3/4)$.

In a similar way a four-modal approximation correspond to approximate the exact pruning front with the values:

$\gamma = \kappa_{11}$ for $\delta \in (0, 1/8) \cup (7/8, 1)$

$\gamma = \kappa_{01}$ for $\delta \in (1/8, 1/4) \cup (3/4, 7/8)$

$\gamma = \kappa_{00}$ for $\delta \in (1/4, 3/8) \cup (5/8, 3/4)$

$\gamma = \kappa_{10}$ for $\delta \in (3/8, 5/8)$

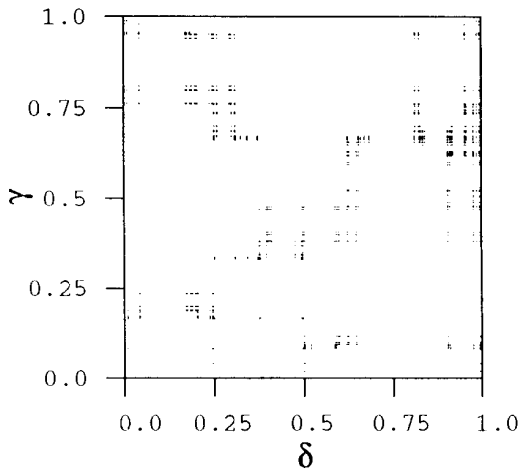

Figure 5.15: A chaotic orbit plotted in symbol space defined by the partition line in figure 5.3 for $a = 1.0$, $b = 0.54$.

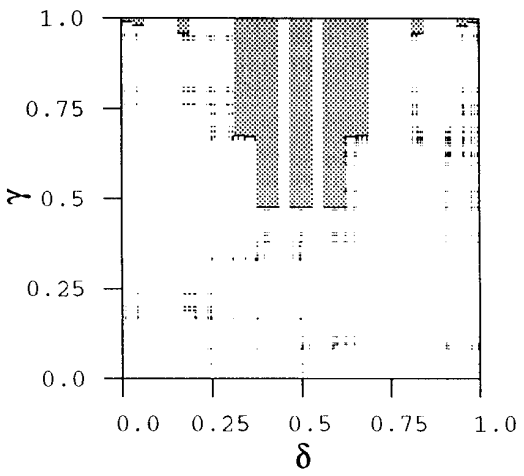

Figure 5.16: The pruning front plotted together with a chaotic orbit in the symbol space for $a = 1.0$, $b = 0.54$

The generalization to any 2^n partition in δ works the same way.

5.3.3 Pruning front for $a = 1.0$, $b = 0.54$

We can construct the pruning front for the chaotic attractor with parameters $a = 1.0$, $b = 0.54$. We use the partition in figure 5.3 which we believe is the unique partition following the role given above. The chaotic orbit gives the points in the symbol plane plotted in figure 5.15.

To construct the pruning front up to a given resolution we have numerically found the primary turning points of the 2^4 or less folds of the unstable manifold that are described by the symbol strings $s_{-4}s_{-3}s_{-2}s_{-1}s_0\cdot$. The symbol s_0 tells whether the point on the fold is to the right or to the left of the primary tangency and it does not distinguish between different folds. The symbol string specify a part of the foliation of the unstable manifold and we choose the primary tangency on the the fold with largest future symbolic value γ.

We find that the following 8 folds have a primary tangency:

$$1110s_0\cdot \quad 0010s_0\cdot \quad 1010s_0\cdot \quad 1000s_0\cdot \quad 0000s_0\cdot \quad 0001s_0\cdot \quad 0111s_0\cdot \quad 1111s_0\cdot \qquad (5.2)$$

while the other 8 folds do not have any primary tangencies. The primary tangency points give respectively the future symbolic values γ; 0.476190, 0.476201, 0.476225, 0.672550, 0.675583, 0.958018, 0.979120, 0.989622. The symbol string $s_{-4}s_{-3}s_{-2}s_{-1}s_0\cdot$ gives 2^5 intervals on the δ axis of length 2^{-5}. For 16 of these intervals which have a primary tangency point we draw the pruning front line and draw

the forbidden region as a gray rectangle above the pruning front line in figure 5.16. The white strips in figure 5.16 is from the 16 intervals on δ which do not have a primary tangency. We do not need a pruning front here because this part of the region is pruned by an image of one of the gray regions. If we want the primary pruned region to be a connected region we can include the white regions above the largest of the two γ values of the neighboring part of the pruning front.

Since the homoclinic tangencies are ordered along the manifolds and the symbol plane has the same ordering as the manifold structure then it follows that the pruning front is monotonously increasing from $\delta = 1/2$ when δ increases or decreases.

5.4 Pruning front for the $|b| = 1$ limit

In the limit of an area preserving map, assuming the symbolic description of orbits is still valid, we have a symmetry between the pruning front and the preimage of the pruning front.

The backward iteration of the Hénon map (4.1) is

$$x_{t-1} = -\frac{1}{b}(1 - ax_t^2 - x_{t+1}) \tag{5.3}$$

If $b = -1$ we have

$$x_{t-1} = 1 - ax_t^2 - x_{t+1} \tag{5.4}$$

This map is the same backward in time as forward in time and interchanging the horizontal and the vertical axis in the phase space plane leaves the non-wandering set unchanged. The non-wandering set and the manifolds are symmetric with respect to the diagonal $x_{t+1} = x_t$. In symbol plane this imply that the points in the non-wandering set are symmetric around the diagonal $\gamma = \delta$. The pruning front is then also symmetric with its preimage. One can think of this preimage as a pruning front of the stable manifold which in this case have to be identical to the pruning front of the unstable manifold.

If $b = 1$ we have

$$x_{t-1} = 1 - ax_t^2 + x_{t+1} \tag{5.5}$$

The sign in front of x_{t+1} has changed and this implies that a point in the non-wandering set is symmetric to a point reflected both around the diagonal and the x_{t+1} axis and this gives $x_{t+1} = -x_t$ as a symmetry line. In the symbol plane the symmetry line is $\gamma = 1 - \delta$. The pruning front is symmetric to its preimage with respect to $\gamma = 1 - \delta$ when $b = 1$. This preimage may be regarded as the pruning front of the stable manifold.

The pruning front is exactly symmetric to its preimage. An approximation of the pruning front with constant γ for intervals of δ of length $2^{-(n+1)}$ is in a general case not symmetric with its preimage because the values of γ will not be equal $m \cdot 2^{-(n+1)}$ with $0 \leq m \leq 2^{(n+1)}$. We can however by using the symmetry identify the cusp bifurcations in a n-approximation which will be at the $b = 1$ or $b = -1$ line.

We can study the isolated cusp bifurcations in the 4-fold approximation of the once-folding map. At the bimodal cusp bifurcation (codimension 2) one period k orbit has two points at the exact pruning front and also two points at the approximated pruning font. We call the cyclic permutations of the symbol string giving κ_{00}: $\overline{S}$, and the permutations giving κ_{10}: $\overline{S'}$. The cusp can be on the $b = -1$ line if

$$\begin{aligned} \gamma(\overline{S}) &= \delta(\sigma^{-1}(\overline{S'})) \\ \delta(\overline{S}) &= \gamma(\sigma^{-1}(\overline{S'})) \\ \gamma(\overline{S'}) &= \delta(\sigma^{-1}(\overline{S})) \\ \delta(\overline{S'}) &= \gamma(\sigma^{-1}(\overline{S})) \end{aligned} \tag{5.6}$$

and on the $b = 1$ line if

$$\begin{aligned} \gamma(\overline{S}) &= 1 - \delta(\sigma^{-1}(\overline{S'})) \\ \delta(\overline{S}) &= 1 - \gamma(\sigma^{-1}(\overline{S'})) \\ \gamma(\overline{S'}) &= 1 - \delta(\sigma^{-1}(\overline{S})) \\ \delta(\overline{S'}) &= 1 - \gamma(\sigma^{-1}(\overline{S})) \end{aligned} \tag{5.7}$$

where σ^{-1} is the inverse shift operation of the symbol string, corresponding to a map once backward in time. This imply that all points in the symbol plane are symmetric to each other with respect to a symmetry line. These symmetric orbits are called the self-adjoint orbits by Mira [153].

The period 4 orbit $\overline{1001}$ gives a cusp for the topological parameter values $\kappa_{00} = \tau(\overline{1001}) = 0.\overline{1110}$ and $\kappa_{10} = \tau(\overline{1100}) = 0.\overline{1000}$. For the two cyclic permutations $\overline{S} = \overline{1001}$ and $\overline{S} = \overline{1100}$ we find

$$\begin{aligned} &\gamma(\overline{1001}) = 0.\overline{1110} = 1 - 0.\overline{0001} = 1 - \delta(\overline{0110}) = 1 - \delta(\sigma^{-1}(\overline{1100})) \\ &\delta(\overline{1001}) = 0.\overline{1011} = 1 - 0.\overline{0100} = 1 - \gamma(\overline{0110}) = 1 - \gamma(\sigma^{-1}(\overline{1100})) \\ &\gamma(\overline{1100}) = 0.\overline{1000} = 1 - 0.\overline{0111} = 1 - \delta(\overline{1100}) = 1 - \delta(\sigma^{-1}(\overline{1001})) \\ &\delta(\overline{1100}) = 0.\overline{0111} = 1 - 0.\overline{1000} = 1 - \gamma(\overline{1100}) = 1 - \gamma(\sigma^{-1}(\overline{1001})) \end{aligned} \tag{5.8}$$

This is the symmetry relation in (5.7) and this cusp is numerically found to be on the $b = 1$ axis, figure 4.31. Several examples of cusps on the $|b| = 1$ lines are given by Mira [153]. Codimension 2 bifurcations in other approximations have a similar symmetry.

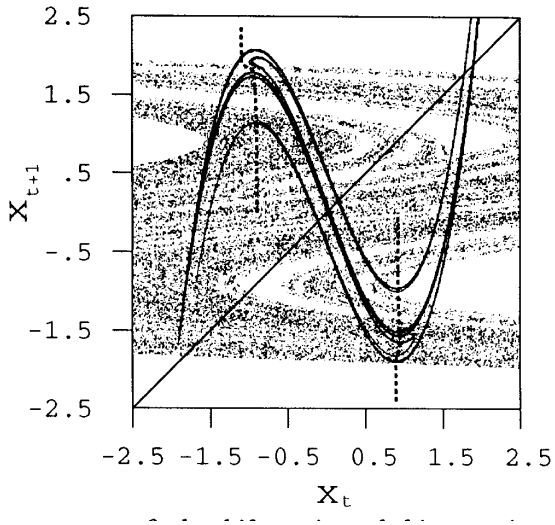

Figure 5.17: The stable and unstable manifolds and the partition lines (dashed lines) for the twice-folding map, $a = 2.55$, $b = 0.1$ and $c = 0.29$.

Codimension 3 and higher bifurcations may also be centered on the $|b| = 1$ line if there are three or more points on the pruning front which have a symmetry around one of the symmetry lines. We do not expect to find a bifurcation of this type in the Hénon map since the Hénon map only has two parameters. As we have seen for the period 8 orbit crossings may a codimension 3 bifurcation structure be revealed in the Hénon map by adding a second parameter.

5.5 Pruning fronts for the twice-folding map

We can also construct the pruning fronts for a n-folding two dimensional map. Each region close to the critical points of the one dimensional map has a partition line through the primary turning points. This give n independent pruning fronts describing the system. We show a numerical example of the pruning front for the twice-folding map (4.55).

The stable and the unstable manifolds are drawn in figure 5.17 for the map (4.55) with $a = 2.55$, $b = 0.1$ and $B = 0.29$. Two partition curves are drawn with dashed lines through the primary turning points in figure 5.17. Also for this twice-folding map we use the rule for changing the partition line defined above for the Hénon map. The difference from the Hénon map to this map is that here the folds A and B in figure 5.5 can go through two different partition lines. The bifurcation of the turning points take place in the same way and the definition of which of the turning points that are primary changes the same way as above. By starting with a complete Smale horseshoe we conjecture that there is a unique partition line.

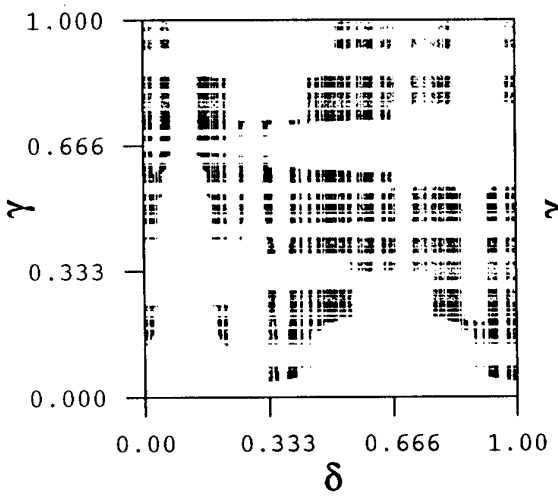

Figure 5.18: The repellor plotted in the symbol plane for $a = 2.55$, $b = 0.1$ and $c = 0.29$.

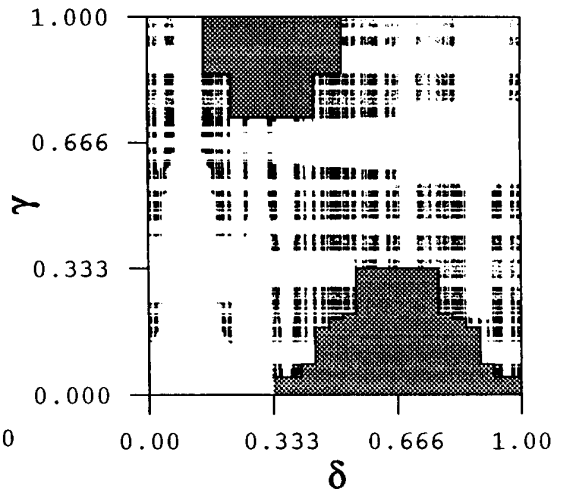

Figure 5.19: The repellor and the two pruning fronts plotted in the symbol plane for $a = 2.55$, $b = 0.1$ and $c = 0.29$.

This map is a pruned version of the flipped twice folded Smale horseshoe in figure 3.15, and the well ordered symbols and the symbolic values (δ, γ) are given in eqs. (3.11) and (3.10). The repellor is drawn in the symbol plane in figure 5.18. We can construct the pruning front by finding the primary turning points, calculate the symbolic description of these and draw the two primary pruned regions. In figure 5.19 the pruning front and the forbidden region is drawn together with the repellor. The two pruning fronts are independent of each other and the two forbidden regions are quite different in this example. We have here chosen to draw the connected primary pruned region.

5.6 Lozi map

The piecewise linear Lozi map (4.3) has a stable manifold W^S and an unstable manifold W^U which also are piecewise linear and are drawn in figure 5.20 for parameter values $a = 1.7$, $b = 0.5$ and for $a = 1.53$ and $b = 0.5$. The analysis of this map is simpler than the Hénon map because W^U has all the primary turning points on the line $x = 0$ and the symbolic description of a point (x_t, x_{t+1}) is given by the sign of x_{t+1}. The pruning front for the Lozi map was also given by Cvitanović, Gunaratne and Procaccia in ref. [53]. The partition and the pruning in the Lozi map has also been studied in detail by D'Alessandro, Isola and Politi [2].

A bifurcation of a primary turning point of the Lozi map is sketched in fig-

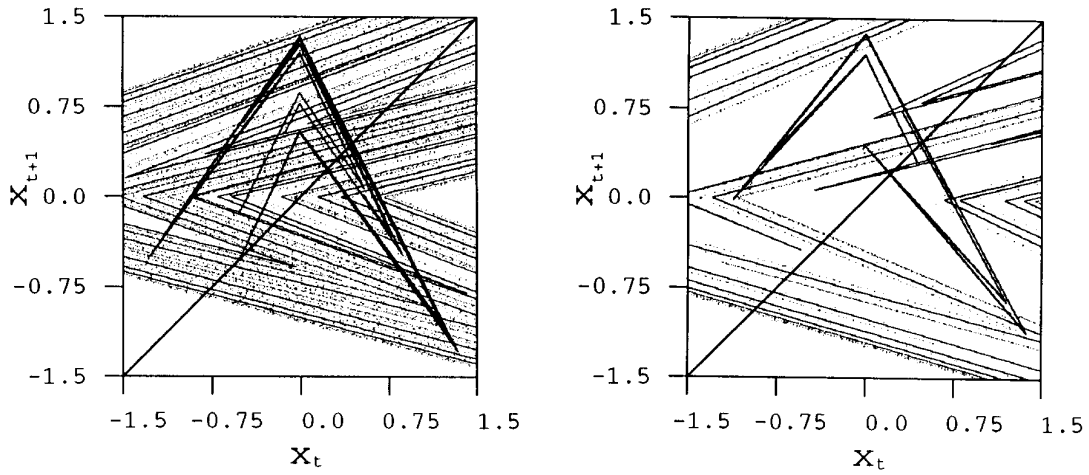

Figure 5.20: The stable and unstable manifolds for the Lozi map, a) $a = 1.7$, $b = 0.5$. b) $a = 1.53$, $b = 0.5$.

ure 5.21. The three points bifurcates together and a jump of the primary turning point is 0. We can not have an isolated cusp in the Lozi map and an orbit does not change symbolic dynamics in a loop in parameter space.

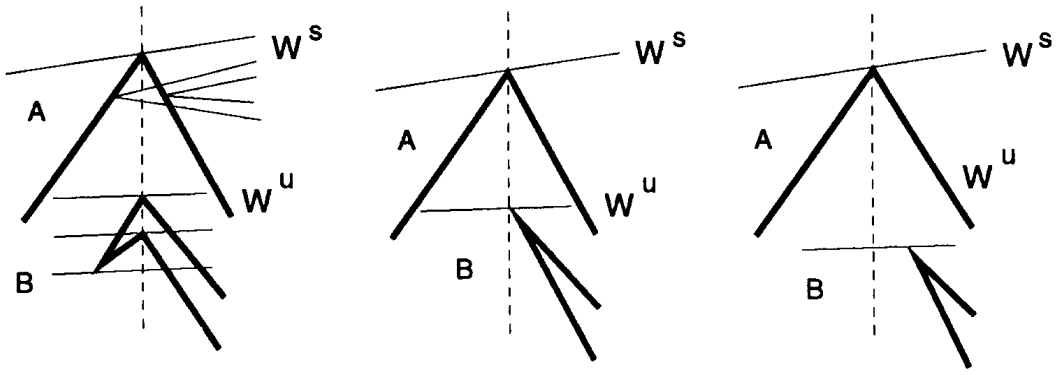

Figure 5.21: The bifurcations of primary turning points in the Lozi map.